Q. J. R. Meteorol. Soc. (2004), **130**, pp. 31–50 doi: 10.1256/qj.03.68

Effects of shear sheltering in a stable atmospheric boundary layer with strong shear

By ANN-SOFI SMEDMAN[1]*, ULF HÖGSTRÖM[1] and J. C. R. HUNT[2]

[1]*Department of Earth Sciences, Meteorology, Uppsala, Sweden*

[2]*Department of Space, Climate Physics and Geological Sciences, University College, London, UK*

(Received 24 October 2002; revised 28 July 2003)

SUMMARY

Data from two marine field experiments in the Baltic Sea with stable stratification have been analysed. The purpose was to test the concept of the 'detached' or 'top-down' eddies and the 'shear-sheltering' mechanism in the presence of a low-level wind speed maximum in the atmosphere. Data used include turbulence and profile measurements on two 30 m towers and concurrent wind profiles throughout the boundary layer obtained from pilot-balloon soundings.

Measurements show that large eddies are being suppressed when there is a low-level wind speed maximum present somewhere in the layer 40–300 m above the water surface and when the stratification is slightly stable. The effect is seen both in normalized standard deviations of the velocity components and in corresponding component spectra. In previous work it was argued that the relatively large eddies, which dominate the low wave number spectra in measurements in the surface layer, are detached or top-down eddies generated higher up in the boundary layer, that interact with the surface layer. The low-level wind maximum introduces a distinct layer with strong vorticity which, according to the shear-sheltering hypothesis, prevents these eddies from penetrating downwards.

In the limit of the wind maximum occurring at a very low height (less than about 100 m), usual turbulence statistics characteristic of the 'canonical' boundary layer are found. Combining all the statistics, it is demonstrated that the wavelength of maximum spectral energy is locally related to a turbulence length-scale, which shows that for values of the Richardson number of unity or less the effect of the local wind gradient is greater than that of static stability. The reduction of length-scale with the strength of a low-level wind maximum, explains the observed reduction (by a factor of two) of the turbulent flux of sensible heat at the surface. This result indicates that the shear-sheltering mechanism is likely to play an important role in the turbulent exchange process at the surface in sea areas where low-level wind maxima are a frequently occurring phenomenon, such as the Baltic and other large water bodies surrounded by landmasses.

KEYWORDS: Low-level jet Stable marine boundary layer Turbulent exchange

1. INTRODUCTION

In previous studies (Smedman *et al.* 1995, 1997) it was shown how the presence of a wind maximum at a low height (40–300 m) above the water surface at two marine sites appears to have strong influence on the turbulence structure of the layer below the jet. The general observed effect is a decrease in energy of relatively large-scale fluctuations, in particular in the horizontal along-wind direction. In Smedman *et al.* (1997) the similarity of the observed phenomena in the atmosphere with so-called shear suppression observed in toroidal plasma confinement devices was discussed (Terry 2000). This plasma turbulence phenomenon is characterized by the simultaneous formation of strong shear, steep gradients of density and temperature, a marked decrease in fluctuation activity, and an increase in the time for which heat and particles are confined in the device. However, no attempt was made to explain the dynamics involved.

If attention is focused on the simultaneous presence of strong shear and suppression of turbulence, an apparent paradox results, because production of turbulence is proportional to the magnitude of the shear, so increased shear would be expected to lead to increased turbulence rather than to 'suppression'. The situation is, however, very different if one considers the fate of eddies which are present in the layer immediately

* Corresponding author: Department of Earth Sciences, Meteorology, Villavägen 16, S-75236 Uppsala, Sweden. e-mail: annsofi@big.met.uu.se

above the strong shear zone and which move towards this zone. As shown by Hunt and Durbin (1999), eddies which move with a horizontal velocity close to that of the mean flow and which have appropriate size are prevented from penetrating through the shear zone—the process of *shear sheltering*.

In section 2 a brief outline of the dynamics of shear sheltering is given, indicating qualitatively which effects would be expected in the atmospheric boundary-layer case with a low-level jet. In section 3 data from two atmospheric experiments are presented and analysed.

2. THEORY

Hunt and Durbin (1999) discuss a wide class of flows characterized by 'interactions between different types of velocity fields that are separated by thin interfacial layers, where there are dynamically significant variations of vorticity across the layers and, in some cases within them'. They argue that, depending on the actual flow situation, two interacting velocity fields may 'resonate with each other and perhaps cause extra turbulence at the interface', or 'mutually exclude each other across the interface'. The latter situation is what the authors term *shear sheltering*. A short introduction to the physics behind the phenomenon is given below, based on the comprehensive text of Hunt and Durbin (1999), and the reader is referred to that paper for details.

The main tool used by Hunt and Durbin (1999) is rapid-distortion theory (RDT, Townsend 1976). Figure 1(a) shows the result of such calculations for a situation which bears some similarity to the atmospheric boundary-layer case. The flow is fully turbulent in the two regions [F1] and [F2], but there is mean shear only in [F2]. The RDT calculations show what happens to detached eddies present in the upper layer which are moving towards the lower region. The graph on the right-hand side of Fig. 1(a) shows that the turbulence statistics change rapidly across the interface between the two regions. Thus the longitudinal velocity fluctuations (circles) increase to a maximum at the interface itself, being very much reduced below the interface. The vertical velocity fluctuations (crosses) are also strongly reduced in [F2] compared to their level in the upper region, although the variation of this quantity is continuous across the interface. The Reynolds stress (line with vees) is seen to change sign at the interface.

The result shown in Fig. 1(a) is valid for eddies moving horizontally with the velocity of the mean flow in the layer immediately above the shear layer. The calculations show that the result is very sensitive to the horizontal velocity of the disturbance and to: 'the timing and sequence in which the different components of the mean and turbulent flow are introduced or generated; this can make the difference as to whether the fluctuations are exclusive, as in shear-sheltering situations, or whether mean shear co-exists with external fluctuations and then slowly interacts with it'.

Hunt and Durbin (1999) introduce an idealized two-dimensional case for which shear sheltering can be studied using simple analytical means, and which can serve the purpose of highlighting the basic dynamics of this phenomenon. An example of how the shear-sheltering mechanism affects interaction between free-stream turbulence and a boundary layer is given by Jacobs and Durbin (1998). As shown in Fig. 1(b)(i), the flow is uniform with speed $U^{[1]}$ in region [F1] above a thin intermediate layer of depth h, and also uniform but with speed $U^{[2]}$, in the layer [F2] below. An eddy with length L is moving horizontally with speed $c = c_r + U^{[S]}$, where $U^{[S]} = \frac{1}{2}(U^{[1]} + U^{[2]})$, and vertically downwards with speed $v^{[1]}$. Figure 1(b)(iii) illustrates schematically how the eddy induces horizontal convergence in the shear zone between [F1] and [F2] at C_u and C_d, and divergence at D_0 as it moves over the interface. Continuity then

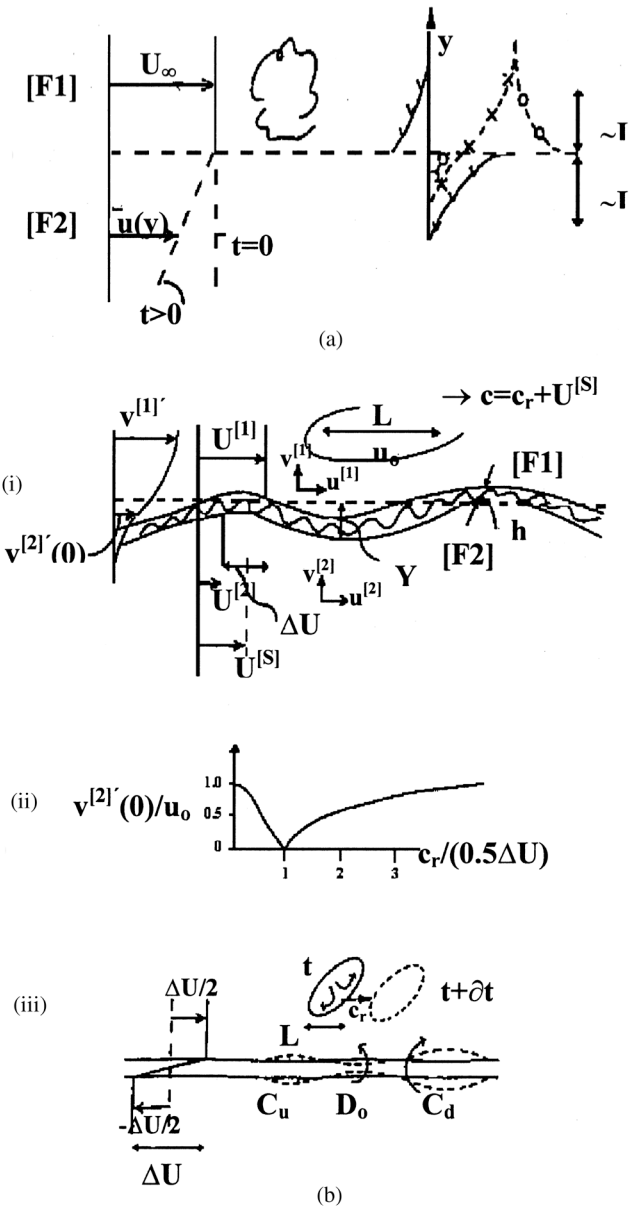

Figure 1. Idealized models of inhomogeneous turbulence dynamics. (a) Large-scale turbulence above a uniform shear layer. Schematic diagram of the interaction between turbulence in region [F1] and the flow in [F2] where a mean shear is initiated when $t > 0$, showing the differences in profiles of the longitudinal velocity variance, $\overline{u^2}$ (lines:-o-o-o), and the vertical velocity variance, $\overline{v^2}$ (lines x-x-x), either side of the interface and the growth of positive and negative Reynolds stress $-\overline{uv}$ for $t > 0$ (-v-v-v). From Hunt and Durbin (1999). (b) Large-scale turbulence above a thin vortex sheet: (i) free stream disturbance in region [F1] travelling near a thin shear layer with a velocity c_r relative to the average velocity $U^{[S]}$ in the layer; (ii) the degree of shear sheltering as defined by the rms vertical velocity fluctuation in region [F2] just below the shear layer, as a function of the ratio of the relative disturbance speed c_r to the velocity jump $\Delta U/2$; (iii) schematic explanation of how a vortex sheet 'blocks' and 'shelters' the velocity induced by an eddy travelling at a relative velocity c_r through strengthening the vortex sheet at convergence points C_u, C_d, and reducing it at the divergence point D_0. From Hunt and Durbin (1999).

requires that there is an upward velocity component as indicated in the figure. Complete shear sheltering is achieved if this velocity equals the downward velocity of the eddy. The requirements for this to happen can be derived with the aid of the vorticity equation (e.g. Batchelor 1967, his Eq. 7.1.5). The strength of the vorticity sheet (the layer between [F1] and [F2]), $\gamma^*(s, t)$, varies both with time, t, and position, s, as the eddy passes by. But $\gamma^*(s, t) = \Gamma + \gamma$, with $\Gamma = -\Delta U$, where $\Delta U = (U^{[1]} - U^{[2]})$ and γ is the change in the strength of the vorticity sheet. For small perturbations, the vorticity equation then becomes to leading order:

$$(\partial/\partial t + U^{[S]}\partial/\partial x)\gamma = -\Gamma \partial u^{[S]}/\partial x,$$

where $u^{[S]}$ is the fluctuating component, which is of order u_0, so that the right-hand side of the equation is of order $U^{[1]}u_0/L$. By a time $t + \delta t$ later, when the vortex has moved by a distance $\delta X = c\delta t$, the vortex sheet at C_d and D_0 has thickened, and thinned, so that the perturbation to the sheet strength is of order $\delta t U^{[1]}u_0/L$. Then an upward perturbation velocity is induced which is comparable to u_0, so that blocking will occur if $\delta t U^{[1]}u_0/L \sim u_0$, provided this velocity is induced at the right place and scale in relation to the velocity of the eddy, i.e. if $\delta X \sim L$. These two conditions for blocking in [F1] and shear sheltering in [F2] are satisfied if $\delta t U^{[1]}/c\delta t \sim 1$, whence $c \sim U^{[1]}$.

Figure 1(b)(ii) shows results of RDT calculations for the ratio $v^{[2]}(0)/u_0$, where $v^{[2]}(0)$ is the vertical velocity fluctuation just below the shear layer, as a function of $c_r/(\frac{1}{2}\Delta U)$. It is seen from the figure that $v^{[2]}(0)/u_0 = 0$ for $c_r/(\frac{1}{2}\Delta U) = 1$. But as $\Delta U = (U^{[1]} - U^{[2]})$ and $U^{[S]} = \frac{1}{2}(U^{[1]} + U^{[2]})$, $c_r/(\frac{1}{2}\Delta U) = 1$ means $c = U^{[1]}$, in agreement with the result obtained above. From Fig. 1(b)(ii) it is evident that effective shear sheltering is restricted to a rather narrow range of values for $c_r/(\frac{1}{2}\Delta U)$. The above derivation is for the case of a two-dimensional eddy. As shown in Hunt and Durbin (1999) the result can, however, easily be extended to apply for a three-dimensional eddy approaching a vorticity sheet as well.

When it comes to possible application of the above ideas to an atmospheric boundary layer with a wind maximum at low level, it is evident from the above discussion (see Hunt and Durbin (1999) for further details) that shear sheltering may occur. But it is by no means certain a priori that this actually happens, because it requires that detached eddies moving with a horizontal speed close to that of the mean flow and having 'appropriate size' (see Hunt and Durbin 1999) are present above the wind maximum. It is also not at all clear from the theory which easily measured parameter(s) should be used to quantify the effect. Figure 2 illustrates schematically the velocity profiles and the corresponding vorticity profiles for the two idealized situations discussed above.

Figure 3 shows an atmospheric case with a low-level wind maximum at about 100 m above the water surface (line with dots). For comparison, a modelled case is also included (the model is described in Bergström (1986)) with the same geostrophic wind, U_g, and approximately the same value for the Monin–Obukhov length, L (for definition see Eq. (A.2)) in the surface layer, but with no low-level wind maximum. (Note that a modelled, rather than a measured, profile has been used for the case without a low-level jet in order to get a profile representing the same combination of U_g and L, as shown in Bergström (1986); the model, which is a straightforward extension of Monin–Obukhov theory, has been successfully tested against atmospheric data for the no-low-level jet case.) As shown in Fig. 3(b), the vorticity is strongly enhanced in the layers below the jet compared to the case without a low-level wind maximum.

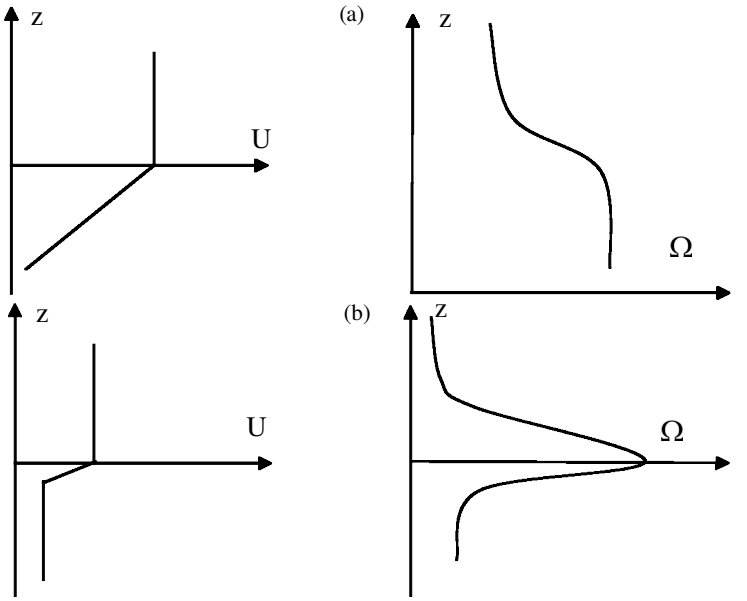

Figure 2. Schematic velocity profiles, left, and corresponding vorticity profiles, right for: (a) large-scale turbulence above a uniform shear layer (same case as in Fig. 1(a)); (b) large-scale turbulence above a thin vortex sheet (same case as in Fig. 1(b)).

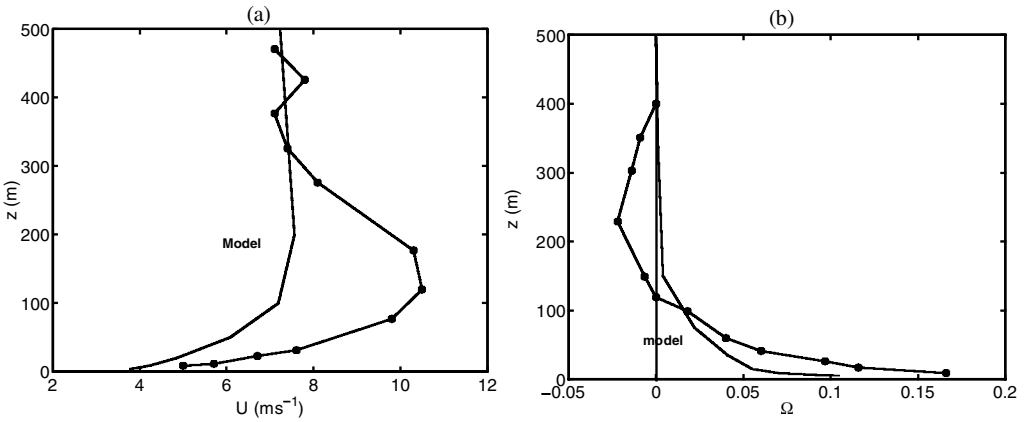

Figure 3. Example wind and vorticity profiles: (a) actual profile for Nässkär 1400 UTC 5 July 1981 with a low-level jet (curve with dots), and a modelled case (Bergström 1986) without a jet but with the same geostrophic wind and roughly the same value of Monin–Obukhov length for the surface layer; (b) corresponding vorticity profiles for actual and modelled wind profiles in (a).

In section 3 data from two marine field experiments are analysed to search for possible evidence of effects from shear sheltering.

3. Results from analysis of atmospheric boundary-layer data

(*a*) *The data*

The data used in this study are taken from two field experiments in the Baltic Sea, performed at the two sites shown in Fig. 4.

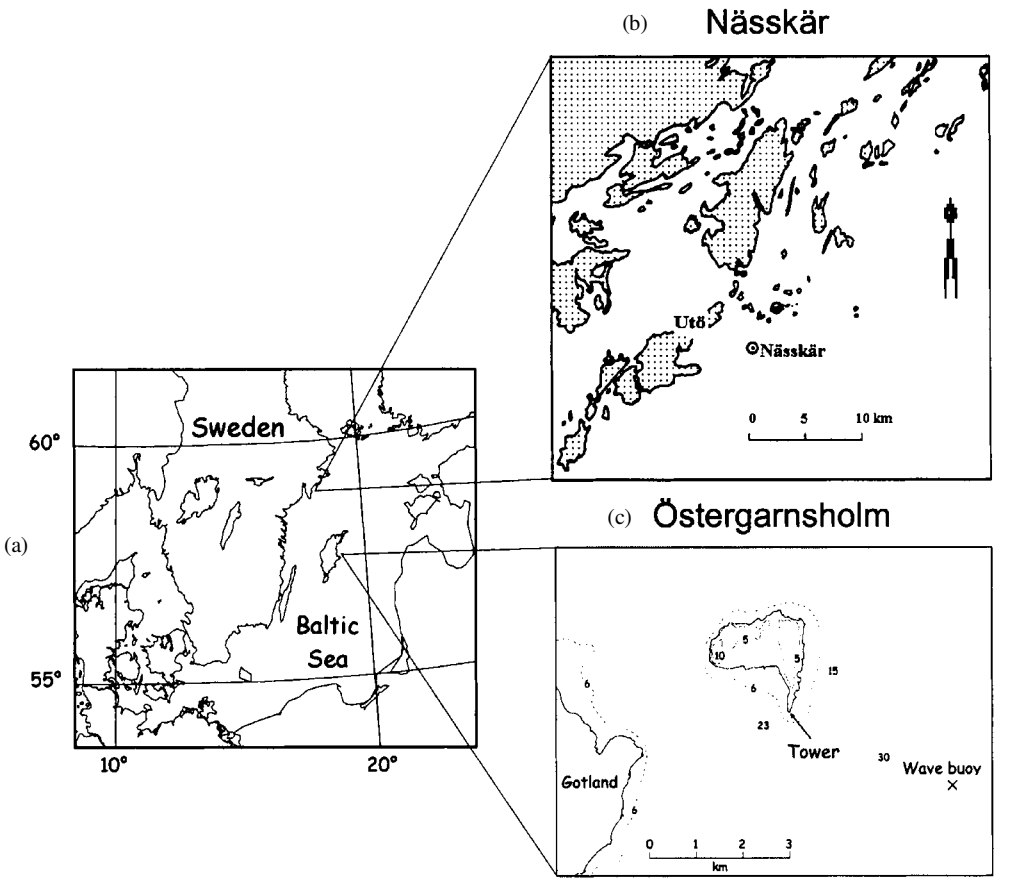

Figure 4. The location of the two marine Swedish measuring sites: Nässkär (58°57′N 18°24′E), situated outside Stockholm and Östergarnsholm (57°25′N 18°59′E) off the east coast of Gotland. Adapted after Smedman *et al.* (1995, 1997).

(i) *Nässkär* (58°57′N 18°24′E) is situated in the outer parts of the Stockholm archipelago; the island is a flat rock of horizontal dimensions 20 × 70 m and maximum height 2 m, with no vegetation. Only data with winds from north-east through south to south-west were used, the over-water fetch for this sector being >100 km. Turbulence measurements with Meteorology Institute Uppsala University (MIUU) instruments (Högström 1982; Bergström and Högström 1987) were made on a tower at 8 and 31 m above mean sea level. This instrument is a wind-vane based, three-axial hot-film probe, with additional sensors for rapid measurement of dry- and wet-bulb temperatures. Additional, slow-response measurements of wind speed and temperature were performed at several levels on the tower; see Bergström and Smedman (1994) and Smedman *et al.* (1995) for further details.

(ii) *Östergarnsholm* (57°25′N 18°59′E) is situated 4 km east of the big island of Gotland; it is flat and covered only with low vegetation; a 30 m tower is sited about 1 m above mean sea level at the southernmost tip of the island. For winds from east to south-west in a clockwise sense, the over-water fetch is >150 km. During the particular period used in this study (May–June 1995) the tower was equipped with a MIUU turbulence instrument at 8 m and with additional slow-response sensors for wind and temperature

at several levels (see Smedman *et al.* (1997) for further details). Also used in the present study are data from radio soundings and pilot-balloon wind measurements from the two sites.

The situations chosen for analysis from the two sites are characterized by a more or less stably stratified boundary layer, and a pronounced wind maximum at a low height, 40–300 m above the surface. For reference purpose, similar situations with no low-level wind maxima are included. All cases represent winds from a sector with more than 100 km undisturbed upwind over-water fetch. Although the situations at the two sites have important similarities—stable stratification and frequent low-level wind maxima—there are also important differences between the two datasets, the Östergarnsholm data representing a generally more strongly stable flow. In addition, conditions at Näsksär were relatively stationary, i.e. the mean fields varied only slowly, the jet being an analogy in space to the well-known nocturnal jet over land. The conditions during the Östergarnsholm May–June 1995 campaign were subject to rapid fluctuations on the mesoscale. These fluctuations were shown by Högström *et al.*(1999) to be the result of two-dimensional stratified turbulence.

(*b*) *Normalized velocity standard deviations and correlation coefficient*

The coordinate system used in the analysis of the atmospheric data differs from that used in section 2, being in accordance with meteorological practice, i.e. the x-axis is along the mean wind, the y-axis is the across-wind component and the z-axis vertical.

In Smedman *et al.* (1995) it was shown (their Fig. 10) that the normalized standard deviation of the longitudinal component, σ_u/u_* (where u_* is the friction velocity), the corresponding lateral component σ_v/u_*, and the vertical component σ_w/u_*, measured at 8 m at Näsksär, all increase with height, h, to the low-level wind maximum. It was noted that the numerical values for these parameters for the case corresponding to the lowest value of $h = 40$ m were close to the corresponding values obtained in flat-plate non-accelerating turbulent boundary layers, the so-called 'canonical' boundary layer. This is consistent with the finding by Jacobs and Durbin (1998) that the shear-sheltering mechanism operates at the level where the curvature of the mean wind profile changes significantly over the eddy-scale. Therefore, the relevant non-dimensional group to assess the strength of this mechanism is

$$\Sigma_J = L_x(\mathrm{d}^2U/\mathrm{d}z^2)/\mathrm{d}U/\mathrm{d}z$$

Since we are focusing on the largest eddies, which at height h are comparable with the boundary-layer height, δ, then $\mathrm{d}U/\mathrm{d}z \sim u_*/\delta$ and $L_x \sim \delta$, so that

$$\Sigma_J \sim \frac{U_{\max}/h^2}{u_*/\delta}, \tag{1a}$$

where $U_{\max}$ is the maximum velocity, which is observed to occur at height h. Thus, $U_{\max}/h^2$ is an approximation for the curvature. A more specific criterion using a local estimated value of $L_x \sim u_*/\mathrm{d}U\ \mathrm{d}z$, is

$$\Sigma_J \approx \frac{U_{\max}/h^2}{(\mathrm{d}U/\mathrm{d}z)^2/u_*}. \tag{1b}$$

Figures 5(a)–(c) show values of σ_u/u_*, σ_v/u_* and σ_w/u_*, respectively, plotted as a function of Σ_J on the ordinate, computed using Eq. (1b), and the flux Richardson number, *Rf*, on the abscissa. The majority of the data points are from the measurements

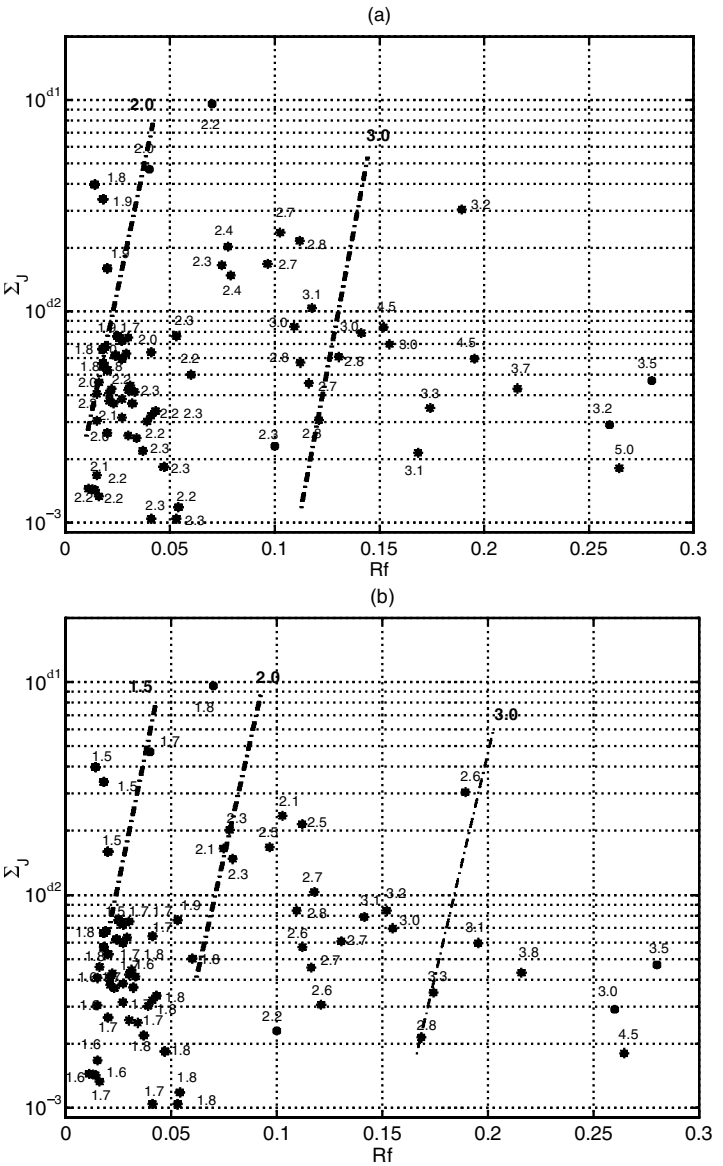

Figure 5. (a) Values of normalized longitudinal velocity standard deviation σ_u/u_* plotted against the flux Richardson number *Rf* on the abscissa, and the bulk profile curvature parameter Σ_J (Eq. (1b)) on the ordinate; (b) as (a), but for the normalized lateral velocity component σ_v/u_*; (c) as (a), but for the normalized vertical velocity component, σ_w/u_*; (d) as (a), but for the correlation coefficient $-r_{uw} = -\overline{u'w'}/\sigma_u\sigma_w$ (values shown are $-r_{uw}$ multiplied by 100). Values for Nässkär are marked as stars, and for Östergarnsholm are given as filled circles. The straight dot-dashed lines in each graph indicate schematically the variation of the particular parameter studied.

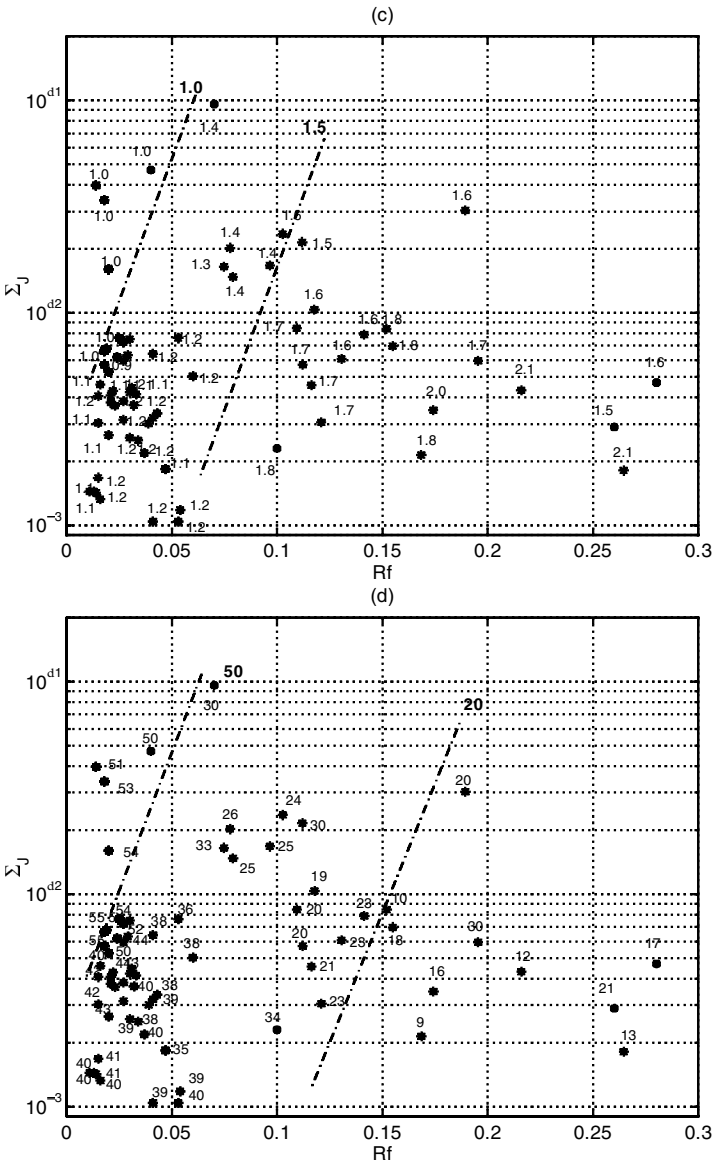

Figure 5. Continued.

at the Nässkär site, but the few data points from Östergarnsholm (see Fig. 5 caption) fit well into the general pattern. It is clear from these graphs that all three normalized standard deviations increase systematically with Rf (as is found in other stratified flows, e.g. Hunt *et al.* (1985)). For $Rf < 0.05$ a certain ordering of the values of the standard deviations with Σ_J is observed for all three components: for small values of Σ_J, $\sigma_u/u_* = 2.2$, $\sigma_v/u_* = 1.7$ and $\sigma_w/u_* = 1.2$, which are to be considered typical values for near-neutral atmospheric conditions; but for larger values of Σ_J all three components are reduced to values typical of the canonical boundary layer, i.e. the flat-plate zero pressure-gradient turbulent boundary layer (see e.g. Andreopolous and Bradshaw 1981)

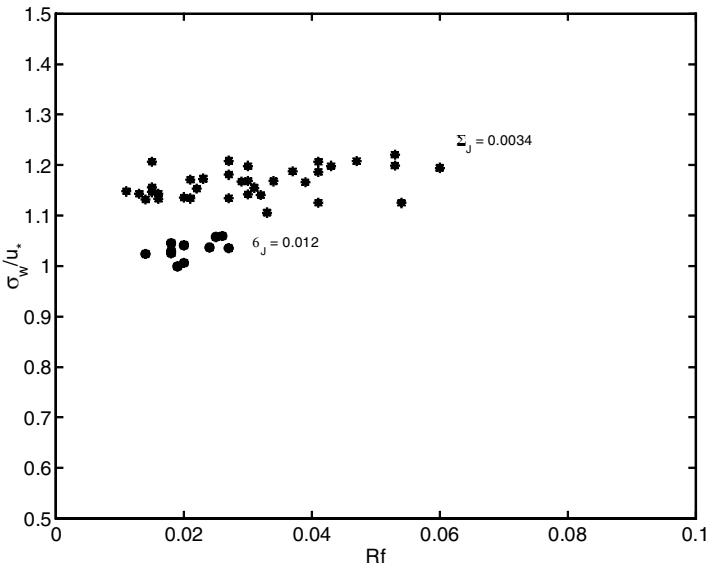

Figure 6. Normalized vertical velocity standard deviation σ_w/u_*, for cases with slightly stable conditions plotted against the flux Richardson number *Rf*. The data, which are from measurements at Nässkär (see Fig. 1), have been divided into two groups according to the value of the bulk profile curvature parameter Σ_J.

$\sigma_u/u_* = 1.9$, $\sigma_v/u_* = 1.5$ and $\sigma_w/u_* = 1.0$. Also the correlation coefficient between u and w, $r_{uw} = \overline{u'w'}/\sigma_u\sigma_w$ attains different values in the neutral atmospheric surface layer where r_{uw} is found to vary between -0.25 and -0.35, from those in the canonical boundary layer where $r_{uw} = -0.50$. Figure 5(d) shows values for r_{uw} plotted against the same variables as the normalized standard deviations. It is found that $-r_{uw}$ decreases systematically with stability. For near-neutral conditions, $r_{uw} \approx -0.40$ for small values of Σ_J and close to -0.50 for large values, in complete agreement with predictions from the shear-sheltering hypothesis.

In Högström *et al.* (2002) it is shown by means of data from ten sites that σ_w/u_* increases systematically with height in the neutral atmospheric surface layer, giving 'typical' values in the range 1.2 to 1.3 (but values in the range 1.1 to 1.5 do occur). The observed variation is shown in that paper to adhere closely to a prediction by Hunt and Morrison (2000), obtained with RDT computations, being a result of detached eddies of relatively large scale impinging onto the surface. This effect is predicted by Hunt and Morrison (2000) to occur when the turbulent Reynolds number, $Re_\tau = u_e L_e/\nu$, is large enough. Here u_e and L_e are a typical eddy velocity and length-scale, respectively, and ν is kinematic viscosity. This is the case in the atmospheric surface layer, for which $Re_\tau \approx 10^6$, but it does not occur in the typical canonical laboratory boundary layer where Re_τ is less than 10^4. In the light of this theory, it is reasonable to interpret the observed reduction of the normalized standard deviations to their canonical values in the case of large values of Σ_J as a result of shear sheltering, which effectively blocks the detached eddies of relatively large scale.

The near-neutral result for σ_w/u_* is shown for a much more restricted range of *Rf* in Fig. 6. Here data from 8 m at Nässkär have been divided into two groups according to the value for parameter Σ_J. It is clear that data with $\Sigma_J = 0.012$ scatter around 1.0, whereas data with $\Sigma_J = 0.0034$ have a value of around 1.2, in general agreement with the result of Fig. 5(c).

(*c*) *Spectral analysis*

Figure 7(a) shows mean spectra for the longitudinal component from Nässkär in the representation introduced by Kaimal *et al.* (1972), i.e. the spectral estimate multiplied by frequency, $nS_x(n)$ has been normalized with the corresponding velocity component variance, σ_x^2, and plotted against normalized frequency, f/f_0, where f_0 is the frequency obtained at the intersection of the inertial subrange asymptote and $nS_x(n)/\sigma_x^2 = 1$.

Kaimal *et al.* (1972) showed that their measured spectra in the stable atmospheric surface layer collapse remarkably well in this representation, implying that the form of the spectra would be independent of height and stability. The 'universal' Kansas curve, suggested by Kaimal *et al.* (1972) is included in Fig. 7(a) as the full line. It is, however, known (Högström *et al.* 2002) that the Kansas spectra analysed by Kaimal *et al.* (1972) were high-pass filtered, and that the low-frequency range of the spectra does not, in fact, collapse in this representation, so we do not expect our spectra to follow the Kansas curve in this range.

The Nässkär spectra have been divided into the two categories: 'No low-level jet' (NoLLJ) and 'Low-jet' (LLJ), as shown in Fig. 7(a). The LLJ curve is the mean of 118 half-hour spectra taken from cases with a wind maximum present at a height between 40 and 300 m above the surface. The corresponding NoLLJ curve is a mean of 56 half-hour spectra when no low-level wind maximum is present. These two mean spectra represent the same measuring height, 8 m, and roughly the same stability range, $0 < z/L < 0.5$ (see below). Thus, considering only traditional local parameters, it would be expected that these curves would coincide with each other, although not with the Kansas curve.

The actual curves do, however, differ considerably in the range $2 \times 10^{-2} < f/f_0 < 4$, where spectral energy is clearly suppressed in the LLJ case. Thus, in spite of the fact that the LLJ curve is much closer to the Kansas curve (full line), the conclusion is that this curve displays suppression of spectral energy. This has the effect that the spectral maximum point moves to a frequency about a decade higher.

One might ask if the big systematic difference between the LLJ and NoLLJ curves could be due to systematic differences in stability among the spectra in the two groups. In fact there is a certain systematic difference. But making the reasonable assumption that increasing stability would tend to reduce the energy of relatively large eddies, the observed difference in stability between the two groups would be expected to act in the opposite direction from what is observed, the LLJ spectra representing a mean z/L of about 0.1 and the NoLLJ spectra a mean z/L of about 0.3. Note that Richardson number $Ri \ll 1.0$, so that shear dominates.

Also in the vertical velocity spectrum, Fig. 7(b), there is a clear effect of spectral energy suppression in approximately the same f/f_0 range as observed in the longitudinal spectrum. Note that in both graphs there is very good collapse of the data from the two groups in the spectral range above about $f/f_0 = 4$.

In Smedman *et al.* (1997) examples of plots of individual spectra from Östergarnsholm are given. The effect of suppression of low-frequency energy is equally clear there as in our Fig. 7, but in addition another significant feature is seen. As is clear from the case shown in Fig. 8, both the longitudinal and lateral velocity spectrum exhibit a pronounced spectral minimum. Analysis of the May–June 1995 dataset from Östergarnsholm reveals that the ratio $nS_u(n)_{\max}/nS_u(n)_{\min}$ appears to be strongly related to the presence of a low-level wind maximum. Unfortunately pilot-balloon soundings from this measuring period at Östergarnsholm are too few to allow a meaningful plot of the spectral ratio to wind profile curvature, analogous to the procedure in subsection 3(b). As shown in Fig. 9 it is, however, found that the ratio of the spectral maximum to the corresponding spectral minimum is closely related to the local wind gradient, the

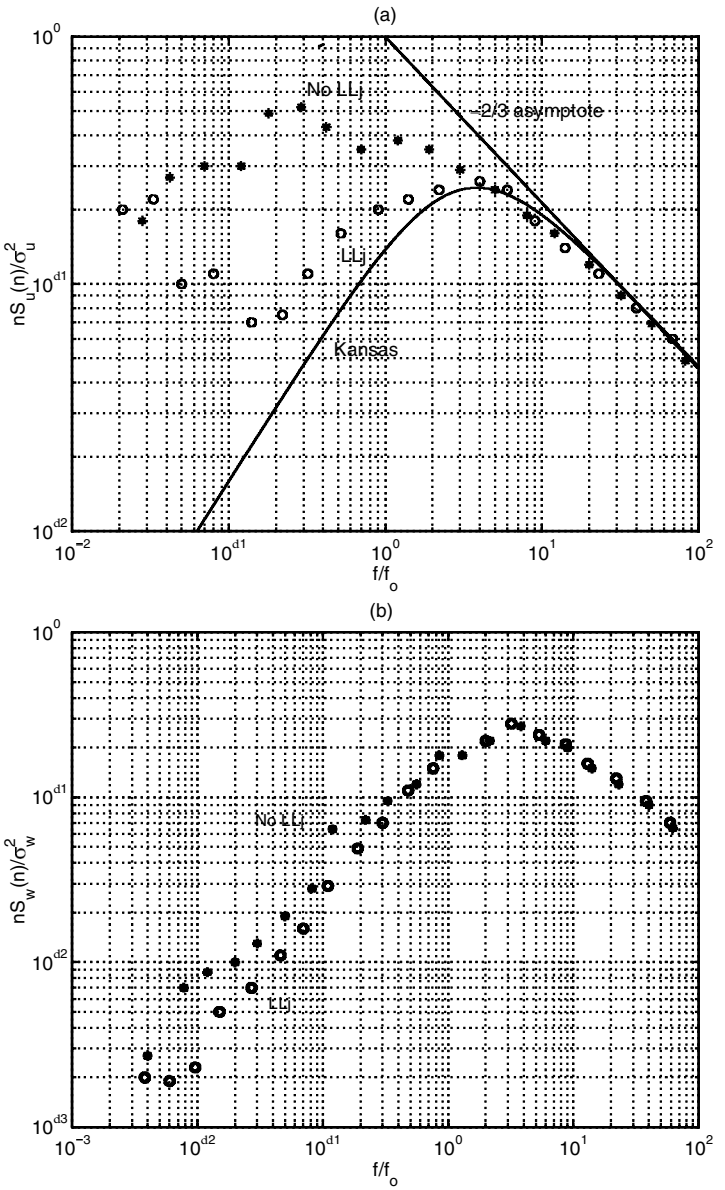

Figure 7. (a) Normalized mean longitudinal velocity spectrum $nS_u(n)/\sigma_u^2$, plotted against normalized frequency f/f_0, where f_0 is the frequency of the intercept between the asymptote to the inertial subrange and $nS_u(n)/\sigma_u^2 = 1$. The data have been divided into two groups: LLJ with a wind maximum present at low levels, and NoLLJ without such a maximum. Also included is the curve (labelled Kansas) suggested by Kaimal *et al.* (1972), their Eq. (23). (b) As (a) but for the vertical component. The LLJ spectrum is the mean of 118 half-hour spectra from 8 m at Nässkär (see Fig. 1) for which $300 > h > 40$ m, where h is the height; the NoLLJ spectrum is the mean of 56 half-hour spectra for NoLLJ cases.

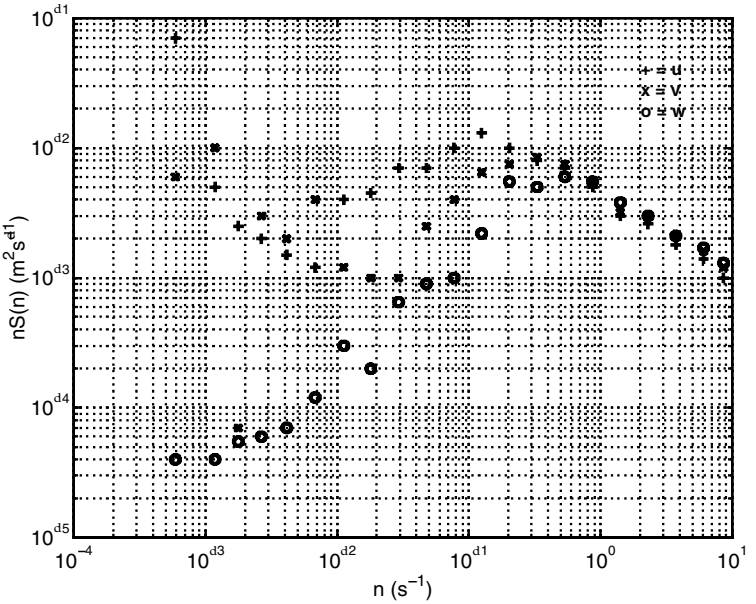

Figure 8. Example of measured wind component spectra during a 30-minute period (1551 UTC 31 May 1995) at Östergarnsholm (see Fig. 1) with fully developed turbulence and a marked spectral gap. Longitudinal component spectra are shown by pluses, lateral component spectra by crosses, and vertical component spectra by circles. Adapted from Smedman *et al.* (1997).

ratio increasing almost linearly in the mean with the magnitude of the wind gradient. The analysis shows further, that no relation to stability is found for this spectral ratio. In view of Fig. 7 it is reasonable to make the hypothesis that the apparent relation seen in Fig. 9 is a manifestation of shear sheltering.

(*d*) *Length-scale analysis*

The observed suppression of low-frequency fluctuations in the spectra (Figs. 7(a), (b) and 8) is observed to result in a systematic increase in the frequency for the spectral maximum. This corresponds to a systematic decrease in the wavelength of the maximum, $\lambda_{\max}$ in the $nS_u(n)$ spectrum. This must be closely related to a corresponding reduction of turbulence integral scales, which are intrinsically related to the forms of the spectra (e.g. Townsend 1976). We now wonder whether this reduction is consistent with the general expression (originating with Riley and Corrsin 1974) for the length-scale $L_z^{(x)}$ in the streamwise direction of the vertical velocity component in this particular type of turbulent shear flows. The general expression that has been proposed for $L_z^{(x)}$ in stratified shear flows is:

$$(L_z^{(x)})^{-1} \approx \frac{A_B}{z} + A_S \frac{\langle \partial U/\partial z \rangle}{\sigma_w}, \tag{2}$$

where A_B and A_S are both of order one and $\partial U/\partial z \neq 0$. The average value of the shear, $\langle \partial U/\partial z \rangle$, is equal to the local value of $\partial U/\partial z$. But in a jet where $\partial U/\partial z = 0$, the average value is taken over the eddy-scale (Hunt *et al.* 1989). In a neutrally stratified, non-accelerating surface layer both terms are comparable. In stably stratified flow, if the buoyancy forces dominate over the shear effect, e.g. wave-like internal motions (Hunt *et al.* 1985), it is pertinent to introduce a length-scale of order σ_w/N (Brost and

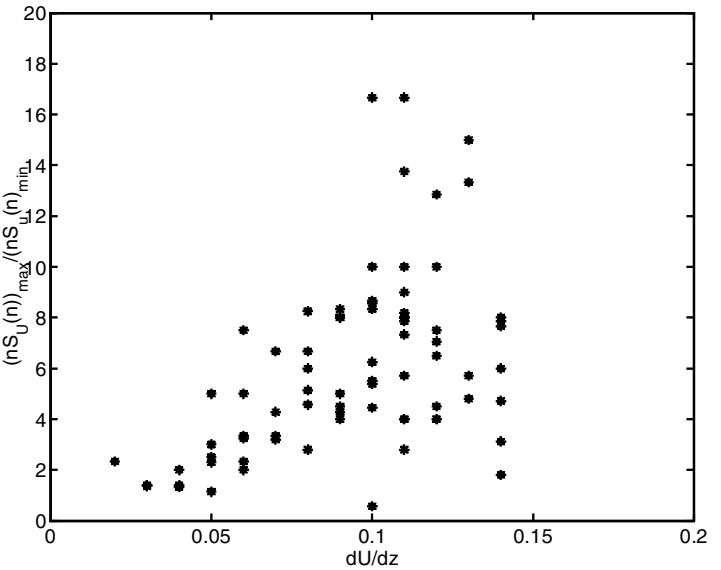

Figure 9. Ratio of the high-frequency maximum in velocity spectrum $S_u(n)$ and the corresponding spectral gap minimum in the same spectrum plotted as function of the wind shear $\partial U/\partial z$. From Smedman *et al.* (1997).

Wyngaard 1978), where

$$N = \sqrt{\frac{g}{T_0}\frac{\partial \Theta}{\partial z}}$$

is the Brunt–Väisälä frequency, with g the acceleration due to gravity, T_0 is the mean temperature in K, and Θ is the mean potential temperature. Thus, for the stably stratified case:

$$(L_z^{(x)})^{-1} \approx \frac{A_B}{z} + A_S\frac{\partial U/\partial z}{\sigma_w} + \frac{B}{(\sigma_w/N)}. \tag{3}$$

Smedman *et al.* (1997) found that for the case of the stable marine boundary layer studied by them, the first term of Eq. (2) can be dropped and, further, that $A_S \approx B \approx 1$, so that denoting the new length-scale by L_{UT}, Eq. (2) becomes:

$$\frac{1}{L_{UT}} = \frac{\partial U/\partial z}{\sigma_w} + \frac{N}{\sigma_w}. \tag{4}$$

In Fig. 10, $\lambda_{\max}$ has been plotted for the longitudinal fluctuations, λ_U against L_{UT}. The graph shows that the wavelength of the maximum in the $nS_u(n)$ spectrum increases nearly linearly with L_{UT}. Note, that the plot is made up of data from both sites (see the legend) and that the two datasets appear indistinguishable. In Fig. 11, $\lambda_{\max}$ has been plotted with separate symbols for all three velocity components. It is seen that all three maximum wavelengths increase linearly with L_{UT}, but with widely differing slopes, indicating strong anisotropy as expected for stably stratified flow.

The parameter L_{UT} combines the effect of shear with the effect of stability. Plots of $\lambda_{\max}$ against each term on the right-hand side of Eq. (4) separately give a pattern similar to that of Figs. 10 and 11 but with more scatter (not shown). In order to quantify this effect, regression analysis was performed for λ_U against, in turn, L_{UT}, σ_w/N and $\sigma_w/\partial U/\partial z$. This analysis was carried out for: (i) all data; (ii) data with $Ri < 0.3$;

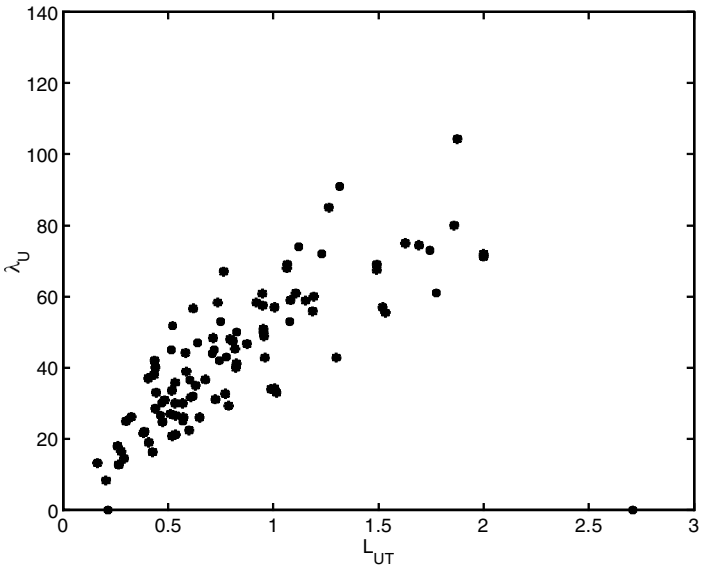

Figure 10. Wavelength at maximum in velocity spectrum $nS_u(n)$ plotted against the length-scale L_{UT} (Eq. (3)). Values for Nässkär are given by stars, and those for Östergarnsholm by filled circles. See Fig. 1 for station locations.

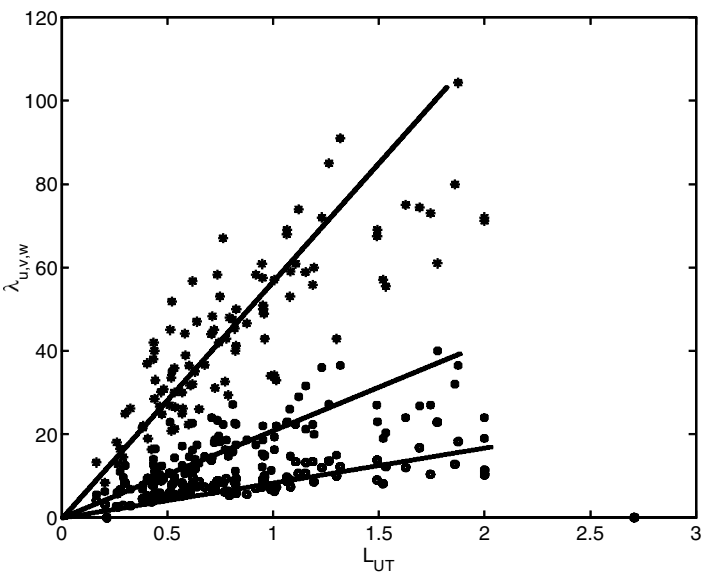

Figure 11. Same as Fig. 10, but for all three velocity components. Longitudinal components are given by stars, lateral components by filled circles, and the vertical components by open circles. Subjective linear fits are also shown for each component.

TABLE 1. STANDARD DEVIATION OF λ_U RELATIVE TO REGRESSION LINES AGAINST VARIOUS ESTIMATES OF MAXIMUM LENGTH SCALES

Ri	L_{UT}	σ_w/N	$\sigma_w/\partial U/\partial z$
All	10.2	12.1	12.9
<0.3	10.8	14.7	10.9
>0.3	9.6	15.0	14.3
<1	10.4	16.2	12.7
>1	7.5	9.7	10.7

λ_U is the wavelength for maximum energy in longitudinal fluctuations; *Ri* is the Richardson number; L_{UT} is the length-scale (Eq. 4); columns 3 and 4 are the individual terms of Eq. (4).

(iii) data with $Ri > 0.3$; (iv) data with $Ri < 1.0$; and (v) data with $Ri > 1$. Table 1 shows the standard deviation of λ_U for each of these cases. It is clear that L_{UT} gives the smallest standard deviation for all five cases. For the least stable cases, $Ri < 0.3$, it is found that the buoyancy term gives a higher standard deviation than the shear term. It is reasonable to attribute the systematic spectral modification seen in Fig. 7 to the first term in Eq. (4) and interpret this as an effect of shear sheltering. This is consistent with Hunt *et al.* (1985).

4. EFFECTS FROM SHEAR SHELTERING ON TURBULENT SENSIBLE-HEAT FLUX IN THE SURFACE LAYER

From the above findings, which show that the large-scale eddies over a fairly wide spectral range are being suppressed, it is reasonable to expect turbulent fluxes in the surface layer also to be influenced by shear sheltering (especially when stable stratification is weak, i.e. $z/L \ll 1$). For the case of the sensible-heat flux, it is convenient to use a bulk formulation, which defines the Stanton number C_H:

$$\overline{w'\theta'} = C_H(U - U_s)(\theta_s - \theta), \tag{5}$$

where $\overline{w'\theta'} = H/\rho c_p$ and H is the sensible-heat flux (W m^{-2}), ρ is air density (kg m^{-3}) and c_p specific heat at constant pressure (J kg^{-1}K^{-1}), U is the wind speed (m s^{-1}) at a reference height z which is usually taken to be 10 m, U_s is the corresponding wind speed at the sea surface, being close to zero; θ_s is sea-surface potential temperature and θ is potential temperature at height z. It is common practice to reduce C_H to the so-called neutral Stanton number, C_{HN}, which is obtained with the following expression (see appendix for a derivation):

$$C_{HN} = \frac{\kappa^2}{\{\ln(z/z_0)\}\{\ln(z/z_{0T})\}}, \tag{6}$$

where von Karman's constant $\kappa = 0.40$, z_0 is the roughness length for momentum and z_{0T} the corresponding roughness length for temperature. As explained in the appendix, z_0 and z_{0T} are obtained from measurements of the momentum flux and the sensible-heat flux, wind speed at 10 m, and the difference between potential temperatures at 10 m and at the sea surface.

Table 2 gives mean values and standard deviation for C_{HN} at Nässkär and Östergarnsholm for May–June 1995. The mean value of 0.64×10^{-3} for the NoLLJ cases at Nässkär is not far from values typically reported for stable conditions (Smith

TABLE 2. NEUTRAL BULK EXCHANGE COEFFICIENT C_{HN} FOR CASES WITH AND WITHOUT A LOW-LEVEL JET

Case	$C_{HN} \times 10^3$	(Standard deviation) $\times 10^3$	No. of data
Nässkär, LLJ	0.30	0.09	12
Nässkär, NoLLJ	0.64	0.11	23
Östergarnsholm	0.43	0.23	50

LLJ refers to cases with a low-level jet and NoLLJ refers to those without. Data are for May–June 1995.

1980; Large and Pond 1982; DeCosmo *et al.* 1996). The mean value for the LLJ cases is less than half of the NoLLJ value, being $0.30.10^{-3}$. The wind speed was in the range 4–8 m s^{-1}, but no systematic variation with wind speed is found in any of the two datasets. The number of cases are limited: 12 for LLJ and 23 for NoLLJ (this large reduction in numbers of data compared to what was used in constructing Figs. 7(a) and (b) is due to the requirement for a valid sea surface temperature (SST) measurement; the SST sensor was very prone to damage by wave action). However, the standard deviation of the C_{HN} estimates in each group is as low as 0.1×10^{-3}, making the difference of the mean values significant. The corresponding data in Table 2 from the spring 1995 Östergarnsholm field campaign has a mean value of C_{HN} of 0.43×10^{-3}. As mentioned previously, we know that low-level wind maxima were common during this field campaign, but the pilot-balloon soundings were too few to allow a strict division of data according to the occurrence/non-occurrence of a low-level wind maximum. The standard deviation for this dataset is double those for each of the two Nässkär datasets. Thus the observed mean and standard deviation are in accordance with what would be expected from the Nässkär data for a combination of roughly equal amounts of LLJ and NoLLJ data.

5. DISCUSSION AND CONCLUSIONS

It is clear from the above analysis of atmospheric data from two marine sites, that when there is a wind maximum present close to the surface ($h < 300$ m), low-frequency turbulent energy in the surface layer is being suppressed relative to that for corresponding cases without such a low-level wind maximum. It is argued that shear sheltering is a mechanism which could explain the experimental findings reported in this paper. Shear sheltering prevents 'detached' eddies generated by the shear in the layers above the wind maximum from penetrating down to the layers near the surface. It has also been demonstrated that this leads to a reduction of the sensible-heat flux at the surface—in the cases studied here the flux was cut to half of that found in NoLLJ cases. The mechanism is similar to that demonstrated by Hunt and Durbin (1999) with the aid of RDT and stability theory, that shear-sheltering effects will occur provided certain requirements are met:

- the horizontal velocity of the detached eddy must be close to the mean speed of the flow above the zone with strong shear;
- the size of the eddy must be appropriate.

It should be noted, however, that the present measurements give no direct information about the detached eddies, which are postulated to be present above the wind maximum.

The observed significant reduction of the sensible-heat flux at the surface when there is a LLJ is relevant for parametrization of the energy balance at the surface in large-scale models in areas where such wind maxima are a common phenomenon, such as the Baltic Sea and other large enclosed seas.

This paper is the first study of how the shear-sheltering mechanism can alter turbulence spectra. This may have implications for load and fatigue calculations for Σ_J in respect of offshore wind farms in coastal waters.

It is possible that shear sheltering is a phenomenon of far-reaching importance in geophysical flows, and it is interesting to speculate about possible further effects. Hunt and Durbin (1999) suggest that shear sheltering is effective in the roughness sublayer of a flow over a rough surface, the strong wind speed gradient preventing large eddies from penetrating down to the surface. Shear sheltering would then also be the cause of the zero-plane displacement effect for flow over rough surfaces. The above authors also refer to several studies of particular mesoscale weather phenomena which appear to be related to shear sheltering. On an even larger scale, it is speculated that the observed inability for cyclones to pass through the strong Antarctic circumpolar jet might also be a case of shear sheltering.

A very interesting case where shear sheltering is clearly *not* effective is in the 'normal' neutral atmospheric surface layer, i.e. the NoLLJ case, for which Högström *et al.* (2002) have shown that detached eddies of surface-layer-scale moving downwards accomplish most of the momentum exchange (together with upward motions on the same scale). In an earlier study by Högström and Bergström (1996) it was found that most of the momentum transport was achieved by organized motions within these surface-layer-scale structures. This means that air of greater than average velocity is brought down to layers near the surface. This is in agreement with the general result that near-equivalence of eddy horizontal velocity and mean velocity is required for shear sheltering to occur. Thus, eddies with rapidly moving air can overcome the effect of strong shear present in the surface layer. Hunt and Morrison (2000) and Hunt and Carlotti (2004) argue that this is possible only if the turbulent Reynolds number is large enough, as in the atmospheric case. In laboratory flows with low and medium *Re*, where the wall turbulence occupies a greater part of the boundary layer, shear sheltering effectively prevents the relatively weaker detached eddies from penetrating to the surface. This results in a boundary layer where turbulence is created near the surface and gradually diffuses upwards, the canonical boundary layer of turbulence text books.

ACKNOWLEDGEMENTS

The work of the first author was made possible by a grant from The Swedish Research Council, Contract G5103-1340/1999. We would like to thank Dr Larry Mahrt from Oregon State University, Corvallis, USA, for valuable comments on the manuscript. JCRH acknowledges support from NERC to the Centre for Polar Observations and Modelling, University College London, and from the J. M. Burgers Centre, Delft University of Technology, the Netherlands.

APPENDIX

Derivation of bulk formulas for the turbulent sensible-heat flux

According to Monin–Obukhov similarity theory, the vertical variation of normalized wind speed and temperature can be expressed as unique functions of the stability parameter z/L:

$$\frac{\kappa z}{u_*}\cdot\frac{\partial U}{\partial z}=\phi_m(z/L),\qquad \frac{\kappa z}{T_*}\cdot\frac{\partial \theta}{\partial z}=\phi_h(z/L), \tag{A.1}$$

where $T_*(= -\overline{w'\theta'}/u_*)$ is the temperature-scale, and L is the Monin–Obukhov length-scale:

$$L = -\frac{u_*^3 T_0}{\kappa g \overline{w'\theta'_v}}. \tag{A.2}$$

Here T_0 is the mean temperature of the surface layer, $\kappa = 0.40$ and $g = 9.81$ m s^{-2}.

Integration of Eq. (A.1) gives mean variables at height z:

$$U(z) - U_s = (u_*/\kappa)\{\ln(z/z_0) - \psi_m\}, \tag{A.3}$$

$$\theta(z) - \theta_s = (T_*/\kappa)\{\ln(z/z_{0T}) - \psi_h\}, \tag{A.4}$$

where z_0 and z_{0T} are the roughness lengths for momentum and heat, at which heights the extrapolated wind speed and temperature approach their surface value U_s and θ_s. U_s is generally not larger than 10^{-2} m s^{-1} and is usually set to zero. ψ_m and ψ_h are the integrated analytical forms of the non-dimensional gradients, ϕ_m and ϕ_h respectively:

$$\psi_m = \int_{z_0/L}^{z/L} \{1 - \phi_m(\zeta)\}/\zeta \cdot \mathrm{d}\zeta, \tag{A.5}$$

$$\psi_h = \int_{z_0/L}^{z/L} \{1 - \phi_h(\zeta)\}/\zeta \cdot \mathrm{d}\zeta, \tag{A.6}$$

where $\zeta = z'/L$.

From Eqs. (4) and (A.4), the bulk exchange coefficient for heat can be written as:

$$C_H = \frac{\kappa^2}{\{\ln(z/z_0) - \psi_m\}\{\ln(z/z_{0T}) - \psi_h\}}. \tag{A.7}$$

Concerning the ϕ_m and ϕ_h functions, expressions from Högström (1996) have been employed:

$$\phi_m = 1 + 5.3z/L, \quad z/L > 0, \tag{A.8}$$

$$\phi_h = 1 + 8.0z/L, \quad z/L > 0. \tag{A.9}$$

According to Eq. (A.7), the transfer coefficient for sensible heat for neutral stratification is:

$$C_{HN} = \frac{\kappa^2}{\ln(z/z_0)\ln(z/z_{0T})}. \tag{A.10}$$

Here, z_0 and z_{0T} are obtained from Eqs. (A.3) and (A.4), with (A.5), (A.6), (A.8) and (A.9).

References

Andreopoulous, J. and Bradshaw, P. 1981 Measurements of turbulence structure in the boundary layer of a rough surface. *Boundary-Layer Meteorol.*, **20,** 201–213

Batchelor, G. K. 1967 *An introduction to fluid dynamics*. Cambridge University Press, Cambridge, UK

Bergström, H. 1986 A simplified boundary layer wind model for practical application. *J. Clim. Appl. Meteorol.*, **25,** 813–824

Bergström, H. and Högström, U. 1987 Calibration of a three-axial fiber-film system for meteorological turbulence measurements. *Dantec Information*, **5,** 16–20

Bergström, H. and Smedman, A. 1994 Stably stratified flow in a marine surface layer. *Boundary-Layer Meteorol.*, **72,** 239–265

Brost, R. A. and Wyngaard, J. C. 1978 A model study of the stably stratified planetary boundary layer. *J. Atmos. Sci.*, **35,** 1427–1440

DeCosmo, J., Katsaros, K. B., Smith, S. D., Anderson, R. J., Oost, W. A., Bumke, K. and Chadwick, H. 1996 Air–sea exchange of water vapor and sensible heat: The Humidity Exchange Over the Sea (HEXOS) results. *J. Geophys. Res.*, **101,** 12001–12016

Högström, U. 1982 A critical evaluation of the aerodynamic error of a turbulence instrument. *J. Appl. Meteorol.*, **42,** 55–78

1996 Review of some basic characteristics of the atmospheric surface layer. *Boundary-Layer Meteorol.*, **78,** 215–246

Högström, U. and Bergström, H. 1996 Organized turbulence structures in the near-neutral surface layer. *J. Atmos. Sci.*, **53,** 2452–2464

Högström, U., Smedman, A. and Bergström, H. 1999 A case-study of two-dimensional stratified turbulence. *J. Atmos. Sci.*, **56,** 959–976

Högström, U., Hunt J. C. R. and Smedman, A. 2002 Theory and measurements for turbulence spectra and variances in the atmospheric neutral surface layer. *Boundary-Layer Meteorol.*, **103,** 101–124

Hunt, J. C. R. and Carlotti, P. 2004 Statistical structure of the high Reynolds number turbulent boundary layer. *Flow, turbulence, combustion*, in press

Hunt, J. C. R. and Durbin, P. A. 1999 Perturbed vortical layers and shear sheltering. *Fluid Dyn. Res.*, **24,** 375–404

Hunt, J. C. R. and Morrison, J. F. 2000 Eddy structure in turbulent boundary layers. *Eur. J. Mech. B–Fluids*, **19,** 673–694

Hunt, J. C. R., Kaimal J. C. and Gaynor, J. E. 1985 Some observations of turbulence structure in stable layers. *Q. J. R. Meteorol. Soc.*, **111,** 793–815

Hunt, J. C. R., Moin, P., Lee, M., Moser, R. D., Spalart, P., Mansour, N. N., Kaimal J. C. and Gaynor, E. 1989 Cross correlation and length scales in turbulent flows near surfaces. Pp. 128–134 in *Advances in turbulence 2.* Second European Turbulence Conference, Berlin, August 1988. Springer Verlag, Berlin, Germany

Jacobs, R. G. and Durbin, P. A. 1998 Shear sheltering and the continuous spectrum of the Orr–Sommerfeld equation. *Phys. Fluids*, **10,** 2006–2011

Kaimal, J. C., Wyngaard, J. C., Izumi Y. and Coté, O. R. 1972 Spectral characteristics of surface-layer turbulence. *Q. J. R. Meteorol. Soc.*, **98,** 563–589

Large, W. G. and Pond, S. 1982 Sensible and latent heat flux measurements over the ocean. *J. Phys. Oceanogr.*, **12,** 464–482

Riley, J. J. and Corrsin, S. 1974 The relation of the turbulent diffusivities to Lagrangian velocity statistics for the simplest shear flow. *J. Geophys. Res.*, **19,** 1768–1774

Smedman, A., Bergström, H. and Högström, U. 1995 Spectra, variances and length scales in a marine stable boundary layer dominated by a low-level jet. *Boundary-Layer Meteorol.*, **76,** 211–232

Smedman, A., Högström, U. and Bergström, H. 1997 The turbulence regime of a very stable marine airflow with quasi-frictional decoupling. *J. Geophys. Res.*, **102,** 21049–21059

Smith, S. D. 1980 Wind stress and heat flux over the ocean in gale force winds. *J. Phys. Oceanogr.*, **10,** 709–726

Terry, P. W. 2000 Suppression of turbulence and transport by sheared flow. *Rev. Mod. Phys.*, **72,** 109–165

Townsend, A. A. 1976 *The structure of turbulent shear flow.* Cambridge University Press. Cambridge, UK